Plasma production in ICRF in the Uragan-2M stellarator in hydrogen-helium gas mixture

V. E. Moiseenko[1,2], Yu. V. Kovtun[1], A. V. Lozin[1], R. O. Pavlichenko[1], A. N. Shapoval[1], L. I. Grigor'eva[1], M. M. Kozulya[1], S. M. Maznichenko[1], V. B. Korovin[1], E. D. Kramskoy[1], N. V. Zamanov[1], Y. V. Siusko[1], D. I. Baron[1], A. Yu. Krasiuk[1], V. S. Romanov[1], I. E. Garkusha[1,2], T. Wauters[3], A. Alonso[4], R. Brakel[5], A. Dinklage[5], D. Hartmann[5], Ye. Kazakov[6], H. Laqua[5], J. Ongena[6], T. Stange[5], and the Uragan-2M Team

[1] Institute of Plasma Physics of the National Science Center "Kharkiv Institute of Physics and Technology", Kharkiv, Ukraine

[2]V.N. Karazin Kharkiv National University, Kharkiv, Ukraine

[3] ITER Organization, St. Paul-lez-Durance, France

[4] Laboratorio Nacional de Fusion, CIEMAT, Madrid, Spain

[5] Max-Planck-Institut für Plasmaphysik, Greifswald, Germany

[6] Laboratory for Plasma Physics, ERM/KMS, Brussels, Belgium

E-mail: Ykovtun@kipt.kharkov.ua

V. E. Moiseenko https://orcid.org/0000-0001-9431-5617; Yu. V. Kovtun https://orcid.org/0000-0003-4948-0896; A. V. Lozin https://orcid.org/0000-0002-8423-0078; R. O. Pavlichenko https://orcid.org/0000-0002-5543-5699; A. N. Shapoval https://orcid.org/0000-0002-4521-7217; M. M. Kozulya https://orcid.org/0000-0003-3854-7047; S. M. Maznichenko https://orcid.org/0000-0002-4548-370X; V. B. Korovin https://orcid.org/0000-0001-8677-1073; E. D. Kramskoy https://orcid.org/0000-0002-3621-468X; Y. V. Siusko https://orcid.org/0000-0002-0789-7100; D. I. Baron https://orcid.org/0000-0001-5971-1243; A. Yu. Krasiuk https://orcid.org/0000-0003-4347-310X; I. E. Garkusha https://orcid.org/0000-0001-6538-6862; T. Wauters https://orcid.org/0000-0002-2941-7817; A. Alonso https://orcid.org/0000-0001-6863-8578; A. Dinklage https://orcid.org/0000-0002-5815-8463; D. Hartmann https://orcid.org/0000-0002-3511-6500; Ye. Kazakov https://orcid.org/0000-0001-6316-5441.

Abstract

Plasma production experiments in helium at Uragan-2M have been performed to investigate the role of the hydrogen minority in helium. The experiments presented here were carried on with a controlled minority hydrogen concentration. The hydrogen minority allowed one to increase plasma density more than three times as compared with pure helium. The obtained plasma density is highest for whole time of Uragan- 2M operation. The developed scenario allowed to decrease the neutral gas pressure at which the plasma production is possible. This is a requirement for achieving regimes of plasma production with full ionization. Although the initial gas mixture 14%H_2+86%He can be treated as optimum, there is no sensitive dependence on hydrogen minority concentration, which makes the scenario robust. This study, together with initial LHD experiments, confirm the prospects of target plasma production by ICRF waves for stellarator type machines.

Keywords: plasma production, ion cyclotron heating, stellarator, Uragan-2M, RF power.

Introduction

The electron-cyclotron resonance heating (ECRH) is the main plasma creation method at Wendelstein7-X (W7-X) [1,2]. After plasma creation, ECRH is used for plasma heating. Plasma is also heated with [1,2] the neutral beam injection (NBI) [1- 3]. Ion-cyclotron resonance heating (ICRH) will be enabled in the next experimental campaigns [2,4].

140 GHz gyrotrons are used at W7-X, and the second harmonic ECRH is realized at the magnetic field of 2.5 T which is, therefore, the regular magnetic field in W7-X experiments. Operation at lower magnetic field of 1.7 T is possible with usage of extraordinary wave ECRH (X3 ECRH) at the 3rd harmonic [5]. The experiments at this magnetic field give an opportunity to investigate high β plasma and more magnetic configurations. The physics of ECR X3- mode heating is also of interest. Calculations [5] show that the X3-mode damping is sufficient for heating if the target plasma has the electron temperature T_e higher than 700 eV and plasma density higher than 10^{13} cm^{-3}. This means, in particular, that X3 ECRH heating cannot be used for plasma production.

X3 ECRH was studied at the Large Helical Device (LHD) [6]. The target plasma was created with the NBI. The NBI can also create target plasma at W7-X. The computations [7] predict that the delay between the NBI start and full neutral gas ionization is about 5 s. During almost whole this time interval the beam shines through. This leads to intolerably high thermal load at the beam dump [8, 9]. The successful NBI plasma creation during less than 0.5 s, the maximum time during which the dump can tolerate the full load, requires initial plasma with a density of 10^{10}-10^{11} cm^{-3} [7]. Other plasma parameters like temperature and ion composition are not so important.

The initial plasma for NBI can be created by the radio-frequency (RF) ICRH system of W7-X. Thus, a possible W7-X plasma operation scenario in the low magnetic field of 1.7 T may consist of the following stages: the initial plasma creation with the RF-discharge; the NBI application for increasing plasma parameters up to the required level; the microwave power heating in the X3 ECRH regime.

A number of experiments were carried out at the Uragan-2M device to research wall conditioning and plasma production scenarios suitable for implementation at W7-X. The two-strap antenna similar W7-X antenna was installed at Uragan-2M to support ICRF experiments at W7-X (wall conditioning, target plasma creation and heating) [10, 11]. The research for plasma creation was carried out with ~100 kW RF power in the helium atmosphere at the pressure of $p = (4 – 14)\times10^{-2}$ Pa [10] at RF frequency near the fundamental hydrogen cyclotron harmonic. It should be noted that the average helium plasma density $(2 – 2.6)\times10^{12}$ cm^{-3} is of the same order as in other RF plasma creation experiments [12, 13].

The scenario of ICRH plasma creation developed at U-2M [10] was examined at LHD [14]. This scenario is attractive since it could use the W7-X ICRH system which is mainly aimed for generation of fast ions. The LHD experimental results show a possibility to use the ICRH plasma creation scenario [10] at large toroidal stellarator type devices.

A small hydrogen minority appeared spontaneously in plasma in above mentioned U-2M experiments [10] was presumably formed via dissociation of the water vapour and hydro-carbons. It was also supplied by the hydrogen which released from the hydrogen pre-loaded inner vacuum surfaces. In such experiments, hydrogen percentage inside plasma wasn’t controlled. It was reasonable to carry out experiments with controlled percentage of H_2 in the H_2+He gas mixture. The information about RF plasma in H_2+He mixtures in literature is mainly related to the RF wall conditioning in tokamaks [14-25] which is normally performed in partially ionized plasma.

The studies described below continue the research of RF discharge in He atmosphere with hydrogen minority which was initiated in [10]. The distinctive feature of these experiments is control over the percentage of hydrogen in the working gas mixture.

Experimental setup and diagnostic methods

The ICRH plasma creation experiments in He atmosphere with H_2 minority were carried out at U-2M stellarator [10, 26,27]. The U-2M photo and scheme are shown in Fig. 1. In this machine, the major torus radius is R = 1.7 m, the minor radius is r_c = 0.34 m and the average plasma radius is r_p < 24 cm.

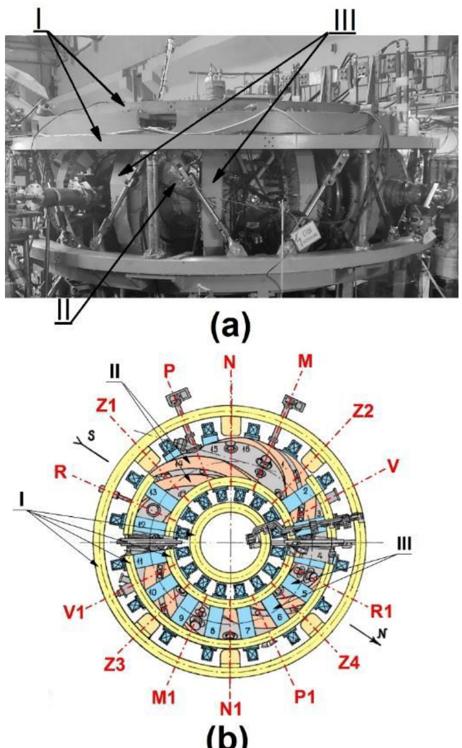

Fig. 1. Photograph (a) and scheme (b) of Uragan-2M. I, II and III respectively poloidal, helical and toroidal (numbered 1–16) field coils. Different toroidal cross-sections are shown by the red lines and denoted by the capital letters and numbers.

The U-2M magnetic system [28,29] consists of the l = 2 helical coils with four periods (m = 4) in the toroidal direction, 16 toroidal field coils evenly distributed along the torus and 8 poloidal coils (see Fig.1). The toroidal magnetic field at the toroidal axis at present is B_0 < 0.6 T ($B_0 = B_{tt}+B_{th}$, B_{tt} and B_{th} are the toroidal fields produced by the toroidal and helical coils respectively,). Magnetic configuration with $K_\varphi \approx 0.32$ is used, where $K_\varphi = B_{th} / (B_{tt}+B_{th})$.

The toroidal vacuum chamber has a volume V_c=3.88 m^3 (without pumping branches). The vacuum chamber is pumped with three turbo-molecular pumps TMN-500 (see fig.1b, cross-sections V, Z1, V1). TMN-500 has maximal pumping speed 0.5 m^3/s for nitrogen gas. The residual gas pressure inside vacuum chamber varies around 1×10^{-5} Pa. The U-2M vacuum system is described in detail in [30].

Plasma is created and heated with the W7-X-like two-strap antenna installed at R1 cross-section (see fig.1b). The antenna consists of two parallel poloidal straps made of stainless steel, 2 mm thick. The strap width is 60 mm, the length is 600 mm, distance between straps ≈ 210mm. It is described in detail in [10, 11]. The antenna is fed in monopole phasing at all the experiments. The antenna is powered by the RF complex Kaskad-1 (K-1) [31]. The RF power value is calculated according to the measurements of the forward and backward waves’ amplitudes inside the feeder line.

The average electron density is measured with the super-heterodyne interferometer at 140 GHz frequency in the R cross-section (see Fig. 1b) [32]. The plasma real-time optical emission spectroscopy was located in the cross-section P1 (see Fig.1b). The emission is recorded with the monochromator-spectrograph SOLAR TII (SOL Instruments Ltd) model MS7501i (Czerny–Turner optical scheme). In N1 cross-section (see Fig. 1b, Fig. 2), the movable cylindrical Langmuir probe measures the ion saturation current. The length of the probe tip is 4 mm and its diameter is 0.8mm.

The U-2M vacuum chamber pressure is measured with vacuum ionization manometers PMI-2 and PMM-32-1. The partial gas pressure inside the vacuum chamber is measured with the mass-spectrometer IPDO-2 (the partial pressure meter of omegatron type OPPM-2) having the omegatron tube RMO-4S (resonant radio frequency mass spectrometer tube). The precision of the residual gases partial pressures measurements is about 25% without calibration. The mass- spectrometer calibration with a single sort pure gas allows one to achieve 10% precision in further measurements. The quantitative gas mixtures analysis took into account the molecular dissociation fragments and the multiply charged ions, which appear during the measurement in the omegatron tube. They are taken into account according to the method described in [33].

The working gases H_2 and He were puffed into vacuum chamber continuously and the flux was controlled with two-channel gas puffing system SNA-2-01. The H_2+He gas mixture experiments are prepared in the following steps: initially, the U-2M vacuum chamber is puffed with helium until a certain pressure, then the hydrogen is additionally puffed into chamber, which increased the pressure in the chamber. The percent ratio of H_2 and He inside the chamber is controlled using IPDO-2 mass-spectrometer measurements. Three experiments were carried out for three different gas mixtures: pure He (with hydrogen appeared spontaneously), 14%H_2+86%He and 25%H_2+75%He.

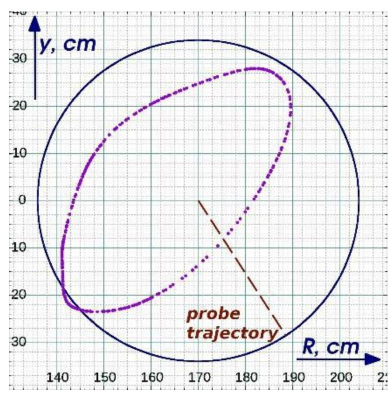

Fig. 2. Head trajectory of single probe (dashed line) in cross-section N1. The magenta dots indicate the last closed flux surface for the magnetic configuration with $K_\varphi = 0.32$.

Experimental Results and Discussions

He discharge.

Two experimental series were carried out for ICRF plasma creation in helium atmosphere. The RF frequency was equal to hydrogen ion-cyclotron frequency in these experiments.

The first experimental series was carried out with constant initial helium pressure p = 0.145 Pa without hydrogen puffing and different anode voltage U_a at the RF generator complex K-1. The experimental conditions were similar to those ones described in the paper [10]. The main goal of this experiment was creating the reference data set. The measurement results are shown in Fig. 3. It is seen that the results of these experiments are in good agreement with previous data [10]. Some difference in the plasma density may be caused by different wall conditions.

The second experimental series was carried out at the RF generator anode voltage U_a = 5–7 kV and initial helium pressure p = 0.145–1.6×10^{-2} Pa. The main goal of these experiments was plasma creation studies at different gas pressures.

The experiments showed that the pressure decrease causes increase of the delay between RF pulse start and the neutral gas breakdown. For example, the times to achieve the average density 5×10^{11}cm^{-3} at the pressure 6×10^{-2} Pa and 3×10^{-2} Pa (U_a = 7 kV) are 6.7 ms and 11.7 ms accordingly. The maximal achieved average plasma density also decreased with the pressure, for example, the average density was less than 1×10^{12}cm^{-3} at p <3×10^{-2} Pa (U_a = 7 kV). At the same time, modulus of reflection coefficient | Γ | inside RF feeder line increased and the power input into antenna decreased accordingly. The anode voltage U_a wasn't set more than 7 kV to prevent arcing at the antenna. It's worth mentioning that similar situation with simultaneous plasma density and He pressure decrease was observed earlier in [12, 13].

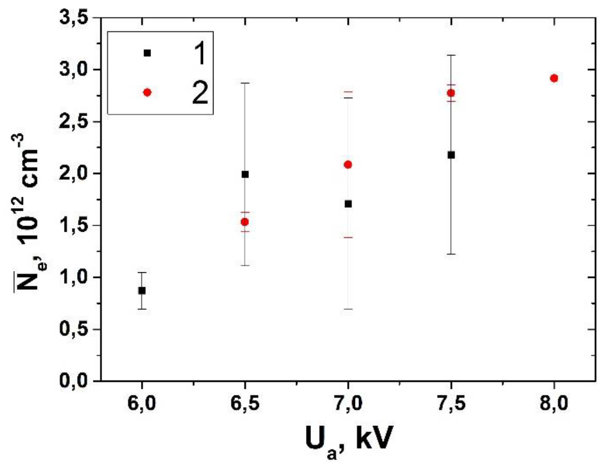

Fig. 3. Maximum average plasma density as a function of the anode voltage on the generator K-1. (Working gas He, p = 0.145 Pa) 1 – experimental data [10], f = 5.15 MHz, B_0 = 0.347 T, K_φ = 0.32, I_{corr} = 470 A, 2 – data of this experimental series f = 4.9 MHz, B_0 = 0.355 T, K_φ = 0.32.

He+H_2 discharge.

The third experimental series was carried out at fundamental hydrogen ion-cyclotron harmonic in mixture of H_2+He. The K-1 generator frequency was f=4.9 MHz, the anode voltage U_a was 7-8 kV. The K-1 timing was: 10 ms (start), 12 ms (step 1), 14 ms (step 2), 22 ms (power off). The anode voltage stepwise grew in this regime ($U_{a1} \approx 0.4\cdot U_a$ start, $U_{a2} \approx 0.6\cdot U_a$ step 1) and reached maximal anode voltage U_a at 14 ms (step 2). Fig. 4 shows the dependencies of the RF power, the average plasma density and different spectral lines intensities. In the plasma density dynamics, several stages. The first stage (t = 10-15 ms) includes preliminary plasma creation and plasma density growth. The RF power is low at this stage due to small antenna – plasma coupling which resulted in almost equal amplitudes of forward and backward waves in the feeder line. The H and He spectral lines intensities increase during this phase. The second phase (t = 15-20 ms) is the further plasma density growth up to $\approx 9\times10^{12}$ cm^{-3}. Owing to the plasma density variation the antenna-plasma coupling changes, and at the end of this stage becomes worse which causes decrease of the coupled power. The He I, He II, H_β spectral line intensities decrease. The third phase is quasi-stationary (t = 20-22 ms), the average plasma density changes in the range of $(7 – 9)\times10^{12}$ cm^{-3}. Note, that O^{+4} (OV) and C^{+4} (CV) spectral lines weren't observed during the shot as well as in Ref. [10]. This is the indication of low electron temperature. The fourth stage begins after the RF heating is off (22 ms). The plasma decay takes place at this phase, the plasma density and spectral lines intensities decrease. At the same time, two stages of plasma density decay time can be distinguished. The average plasma density decreases from 8.3×10^{12} cm^{-3} to 5×10^{12} cm^{-3} for ~ 0.6 ms during the first stage. The He I and He II spectral lines intensities decrease to the minimum for ~ 0.2 ms and ~ 1.2 ms accordingly. The plasma density decreases from 5×10^{12} cm^{-3} to 1×10^{12} cm^{-3} for during ~ 12.9 ms at the second stage. The He I spectral line intensity increases a bit at t = 26ms. This can be explained with electron temperature decrease and helium recombination. The difference between average density decay stages prompts on different loss mechanisms of the charged particles.

These experiments with H_2+He mixture showed that, firstly, the gas breakdown and plasma creation are possible at lower pressure than in pure He while the RF power is the almost same. Secondly, the in the H_2+He mixture the average plasma density is definitely higher than in pure He. Fig. 5 compares the plasma density time evolution for pure He and 25% H_2+75% He mixture. The RF power of about ~ 90 kW created plasma with the average density about ~2.6 times higher then in pure helium. At the same time, the initial gas pressure was ~ 20 times lower than for the pure He discharge. That means that the plasma density increases both with the ionization degree of the neutral gas while the input RF power stays comparable.

The main processes at plasma creation are the neutral gas ionization processes. The neutral gas atoms and molecules electron collision ionization has the threshold nature and is determined with ionization potential U_i [34]. The H_2 molecule (U_i=15.4 eV) and hydrogen atom H (U_i=13.6 eV) have lower ionization potential than helium atom (U_i=24.6 eV). The electron impact ionization cross-section is higher for H_2 and H than for He. For example, the ionization cross-section for H and He atoms at the electron energy E_e = 100 eV is 5.4×10^{-17} cm^2 and 3.65×10^{-17} cm^2 accordingly [35]. The He^+ ion ionization cross-section (U_i = 54.4 eB) is 3.75×10^{-18} cm^2 at E_e=100 eV [36]. The total ionization cross-section for H_2 molecule is 9×10^{-17} cm^2 at E_e=100 eV [37], the partial cross-sections of H_2^+ and H^+ ions formation are 8.24×10^{-17}cm^{-2} and 7.59×10^{-18} cm^{-2} accordingly. So, the ionization of hydrogen is every time faster than helium.

On decrease of the gas pressure, electron collision rate with atoms (molecules) decreases. As a result, there is a minimum gas pressure for successful plasma production. In this case, the hydrogen admixture allows one to soften ionization and breakdown conditions, therefore breakdown pressure is lower than in pure helium. This was observed in the current experiments when the dense plasma was created in H_2+He mixture at lower pressure than in helium (Fig. 5).

The Langmuir probe ion saturation current radial dependence was measured and is shown in Fig. 6, in the capture to which the experimental conditions are listed. The maximal saturation current was observed at the central area *r*~4 cm. The current considerably decreases further with the distance from the center from ~72 mA (*r* = 3 cm) to ~ 4 mA (*r* = 12 cm). The current decreased slower after *r* = 12 cm down to ~ 0.2 mA (*r* = 20 cm). So the mostly dense plasma is observed inside the confinement volume. This is an indication that the electron density profile isn't hollow.

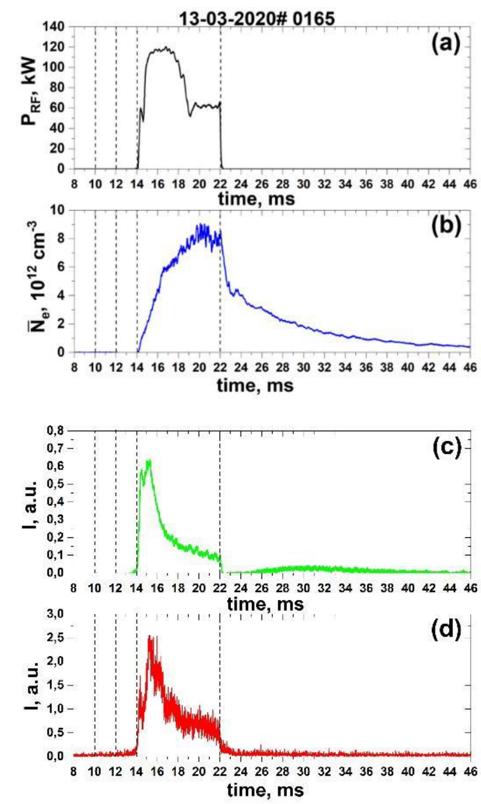

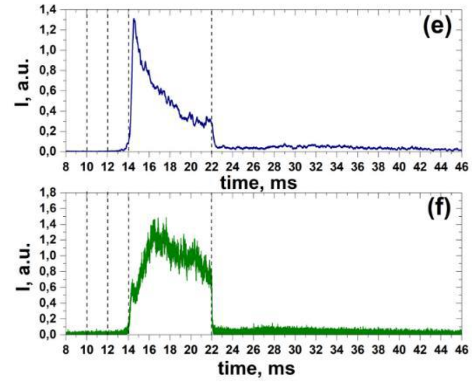

Fig. 4. Time evolutions of RF power (a); average plasma density (b); optical emission intensities of He I, 447.15 nm (c); He II, 468.6 nm (d); H_β, 486.1 nm (e); H_Δ, 410.1 nm (f) (U_a = 8 kV, f = 4.9 MHz, B_0 = 0.341 T, K_φ = 0.32, Working gas 86%He+14%H_2, p = 8.3×10^{-3} Pa). Duty cycle: 10 ms (start), 12 ms (step-1), 14 ms (step-2), 22 ms (shutdown).

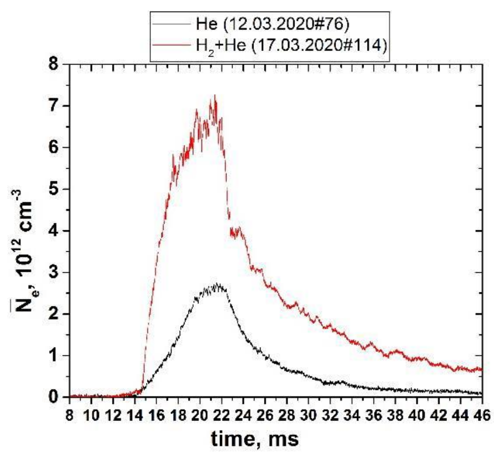

Fig. 5. Time evolutions of average plasma density for He and gas mixture 25%H_2+75%He. (pressure He p = 0.106 Pa, U_a = 7.5 kV, B_0=0.344 T, K_φ = 0.319, f = 4.9 MHz; pressure 25%H_2+75%He p = 5.4×10^{-3} Pa, B_0=0.346 T, K_φ = 0.319, f = 4.9 MHz).

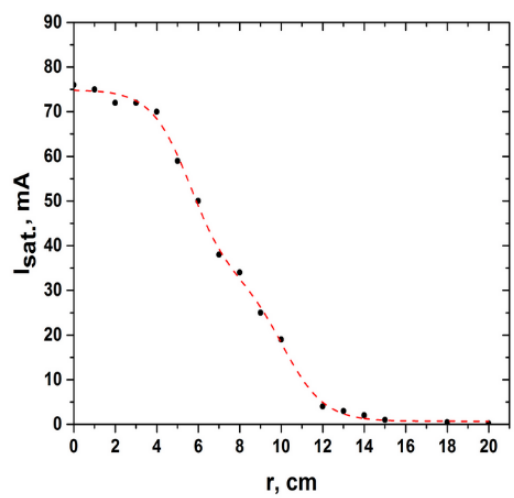

Fig. 6. Dependence of the saturation ion current of the Langmuir probe on the distance between the probe head and the torus axis (see Fig. 2). (gas mixture 14%H_2+86%He, p = 8.3×10^{-3} Pa, f = 4.9 MHz, B_0 = 0.341 T, K_φ = 0.32, U_a = 7.5 kV, t ≈20 ms).

The Fig. 7 shows the dependence of the maximal value of the average plasma density during shot on K-1 generator anode voltage. The plasma density for 25%H_2+75%He initial gas mixture didn't exceed 4.7×10^{12} cm^{-3} at 7 kV voltage. The maximal plasma density value was 8.9×10^{12} cm^{-3} (initial gas mixture 14%H_2+86%He) and was achieved at 8 kV voltage. This value is approximately two times bigger than the average plasma density achieved earlier in U-2M experiments.

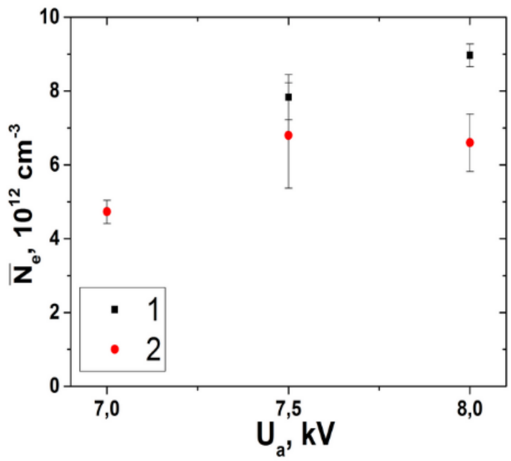

Fig. 7. Dependence of maximum average plasma density as a function of the anode voltage on the generator K-1.

1 – Working gas 86%He+14%H_2, $p = 8.3\times10^{-3}$ Pa, $f = 4.9$ MHz, $B_0 = 0.341$ T, $K_\varphi = 0.32$.

2 – Working gas 75%He+25%H_2, $p = 5.4\times10^{-3}$ Pa, $f = 4.9$ MHz, $B_0 = 0.346$ T, $K_\varphi = 0.319$.

It worth mentioning that the RF experiments on plasma production in tokamaks aimed for vacuum wall conditioning in H_2+He mixture achieved average plasma density of about 10^{10}-5×10^{11} cm^{-3} [15-17, 20]. The first LHD experiments on ICRH plasma creation [14] used the minority scenario [10]. The experiments in ~81%He+19%H_2 ($p = 2.56\times10^{-5}$ Pa) mixture achieved the average plasma density ≈ 9.5×10^{11} cm^{-3} with RF power up to 200 kW. The LHD is much bigger than U-2M and such RF power is probably too small. The RF power density was about 150 kW/m^3 for Uragan-2M experiment and about 7 kW/m^3 for LHD.

Summary and Conclusions

In the experiments at U-2M for plasma production [10] there was made a suggestion on the crucial role of hydrogen which appears in the discharge spontaneously as an impurity. The experiments presented here were made to clarify this suggestion. They were performed in helium with a controlled concentration of the hydrogen minority.

The experimental results directly confirm the above suggestion. Adding a hydrogen minority allowed one to more than triple the plasma density as compared with pure helium. Moreover, it allowed to decrease the neutral gas pre-fill pressure at plasma breakdown, which is necessary to obtain full ionization. Plasma characterization by probes reports on a volumetric and fully ionized plasma discharge. The obtained plasma density was maintained highest for whole time of U-2M operation. Although the initial gas mixture 14%H_2+86%He can be treated as optimum, there is no sensitive dependence on hydrogen minority concentration in the range of 14% to 25%, which makes the scenario robust.

The plasma density achieved in this scenario is 9×10^{12} cm^{-3} which is sufficient for further NBI application and fast discharge development without overheating of the NBI dump. The RF power applied is below 120 kW.

This study, together with initial LHD experiments [14], confirm the prospects of the target plasma production method with ion minority for stellarator type machines.

Acknowledgements

This work has been carried out within the framework of the EUROfusion Consortium and has received funding from the Euratom research and training programme 2014–2018 and 2019–2020 under Grant Agreement No. 633053. The views and opinions expressed herein do not necessarily reflect those of the European Commission.

This work also received funding from National Academy of Sciences of Ukraine (Grants П-3-22, and A-5-20).

Data availability

The datasets generated during and analysed during the current study are available from the corresponding author on reasonable request.

References

[1] T. Klinger et al., Nucl. Fusion **59,** 112004 (2019). https://doi.org/10.1088/1741-4326/ab03a7
[2] M. Endler et al., Fusion Eng. Des. **167,** 112381 (2021). https://doi.org/10.1016/j.fusengdes.2021.112381
[3] S. A. Lazerson et al., Nucl. Fusion **60,** 076020 (2020). https://doi.org/10.1088/1741-4326/ab8e61
[4] D. A. Castano Bardawil et al., Fusion Eng. Des. **166,** 112205 (2021). https://doi.org/10.1016/j.fusengdes.2020.112205
[5] N. B. Marushchenko et al., EPJ Web Conf. **203,** 01006 (2019). https://doi.org/10.1051/epjconf/201920301006
[6] T. Shimozuma et al., Nucl. Fusion 55, 063035 (2015). https://doi.org/10.1088/0029-5515/55/6/063035
[7] D. Gradic et al., Nucl. Fusion **55,** 033002 (2015). https://doi.org/10.1088/0029-5515/55/3/033002
[8] S. Äkäslompolo et al., JINST **14,** P07018 (2019). https://doi.org/10.1088/1748-0221/14/07/P07018
[9] Paul van Eeten et al., Fusion Eng. Des. **146,** 1329 (2019). https://doi.org/10.1016/j.fusengdes.2019.02.069
[10] V. E. Moiseenko et al., J Plasma Phys. **86,** 905860517 (2020). https://doi.org/10.1017/S0022377820001099
[11] A. V. Lozin et al., Probl. At. Sci. Technol. Ser.: Plasma Phys. **6,** 10 (2020). https://doi.org/10.46813/2020-130-010
[12] R. Brakel et al., J. Nucl. Mater. **290,** 1160 (2001). https://doi.org/10.1016/S0022-3115(00)00554-7
[13] H. G. Esser et al., J. Nucl. Mater. **241,** 861 (1997). https://doi.org/10.1016/S0022-3115(97)80155-9
[14] S. Kamio et al., Nucl. Fusion **61,** 114004 (2021). https://doi.org/10.1088/1741-4326/ac277b
[15] A. Lyssoivan et al., J. Nucl. Mater. **337–339**, 456 (2005). https://doi.org/10.1016/j.jnucmat.2004.07.060
[16] A. Lyssoivan et al., *J. Nucl. Mater.* **363–365,** 1358 (2007). https://doi.org/10.1016/j.jnucmat.2007.01.186
[17] M. K. Paul et al., AIP Conf. Proc. **1187,** 177 (2009). https://doi.org/10.1063/1.3273722
[18] G. Sergienko et al., J. Nucl. Mater. **390–391,** 979 (2009). https://doi.org/10.1016/j.jnucmat.2009.01.252
[19] T. Wauters et al., AIP Conf. Proc. **1187,** 173 (2009). https://doi.org/10.1063/1.3273721
[20] A. Lyssoivan et al., J. Nucl. Mater. **390–391,** 907 (2009). https://doi.org/10.1016/j.jnucmat.2009.01.233
[21] D. Douai et al. J. Nucl. Mater. **415,** S1021 (2011). https://doi.org/10.1016/j.jnucmat.2010.11.083
[22] A. Lyssoivan et al., J. Nucl. Mater. **415,** S1029 (2011). https://doi.org/10.1016/j.jnucmat.2010.11.059
[23] Yu. Yaowei et al., Plasma Phys. Control. Fusion **53,** 015013 (2011). https://doi.org/10.1088/0741-3335/53/1/015013
[24] P. Ya. Burchenko et al., JETP Letters **15,** 174 (1972).
[25] T. Wauters et al., Plasma Phys. Control. Fusion **53** 125003 (2011). https://doi.org/10.1088/0741-3335/53/12/125003
[26] V. E. Moiseenko et al., Ukr. J. Phys. **62,** 311 (2017). doi: 10.15407/ujpe62.04.0311
[27] V. E. Moiseenko, Yu. V. Kovtun and I. E. Garkusha, Probl. At. Sci. Technol. Ser.: Plasma Phys. **1,** 3 (2021). https://doi.org/10.46813/2021-131-003
[28] V. Bykov et al., *Fusion Technology*. **17,** 140 (1990). https://doi.org/10.13182/FST90-A29177
[29] O. S. Pavlichenko, Plasma Phys. Control. Fusion **35,** B223 (1993). https://doi.org/10.1088/0741-3335/35/SB/018
[30] G. P. Glazunov et al., Fusion Eng. Des. **170,** 112716 (2021). https://doi.org/10.1016/j.fusengdes.2021.112716
[31] V. B. Korovin and E. D. Kramskoy, Probl. At. Sci. Technol. Ser.: Plasma Phys. **6** 19-21 (2012).
[32] R. O. Pavlichenko, N. V. Zamanov and A. E. Kulaga, Probl. At. Sci. Technol. Ser.: Plasma Phys. **1,** 257 (2017).
[33] G. L. Saksaganski et al., Ultrahigh Vacuum in Radiophysical Apparatus Building (Atomizdat, Moscow, 1976) (in Russian).
[34] J. B. Hasted, Physics of Atomic Collisions. (London, Butterworths, 1964).
[35] Y. Itikawa (ed), Landolt–Börnstein, Group I Elementary Particles, Nuclei and Atoms 17A (Interactions of Photons and Electrons with Atoms) (Berlin, Springer, 2000).
[36] Y. Itikawa (ed), Landolt–Börnstein, Group I Elementary Particles, Nuclei and Atoms 17B (Collisions of Electrons

with Atomic Ions) (Berlin, Springer, 2001).
[37] Jung-Sik Yoon et al., J. Phys. Chem. Ref. Data **37,** 913 (2008). https://doi.org/10.1063/1.2838023